Optical coherent backscattering by random media : an experimental study

P.E. Wolf, G. Maret, E. Akkermans, R. Maynard

Classification
Physics Abstracts
42.20Y — 71.55J — 78.90

Optical coherent backscattering by random media : an experimental study

P. E. Wolf, G. Maret ([1]), E. Akkermans and R. Maynard

Centre de Recherches sur les Très Basses Températures, Centre National de la Recherche Scientifique, avenue des Martyrs, B.P. 166X, 38042 Grenoble Cedex, France
([1]) Hochfeld Magnetlabor, Max-Planck Institut für Festkörperforschung, B.P. 166X, 38042 Grenoble Cedex, France

(*Reçu le 15 juillet 1987, accepté le 22 septembre 1987*)

Résumé. — Nous présentons une étude détaillée de la rétrodiffusion cohérente de la lumière par des suspensions aqueuses de microbilles de polystyrène. Nous discutons particulièrement les effets, sur la forme et la hauteur du pic de rétrodiffusion, de la taille des particules, de l'absorption — contrôlée par l'addition d'un colorant — et de la polarisation de la lumière. Lorsque les polarisations incidente et détectée sont parallèles, la théorie de diffusion scalaire, caractérisée par le libre parcours moyen de transport l^*, rend compte de la forme du pic jusqu'à des angles de (rétro)diffusion étonnement élevés ($ql^* \approx 1$) et de son arrondissement progressif en présence d'absorption. Nous n'observons aucune déviation à la statistique gaussienne habituelle pour le champ diffusé, et ce jusqu'à des rapports $\lambda/l^* \sim 0{,}1$.

Abstract. — A detailed experimental study of coherent backscattering of light from aqueous suspensions of polystyrene microspheres is presented. Emphasis is on the effects of particle size, of absorption due to added dye and of light polarization on the shape and height of the backscattering cone. For parallel polarization of incident and scattered beams, the scalar diffusion theory, parametrized by the transport mean free path l^*, agrees well with our data up to surprizingly large scattering angles ($ql^* \approx 1$) and quantitatively accounts for the rounding of the cones due to absorption. No deviations from the usual Gaussian statistics of scattered fields is observed up to $\lambda/l^* \sim 0.1$.

1. Introduction.

Recently, the intensity of light multiply scattered from ensembles of disordered particles has been found to be enhanced in the backscattering direction [1-6]. This effect occurs both for colloidal suspensions [1-3] and solid samples [4-6]. As in the former case the scattering mean free path could be varied by changing the particle's concentration, it was clearly demonstrated that the enhancement is due to the so-called coherent backscattering (CB) effect [7-10]. This is a general effect in the multiple scattering of waves by a disordered medium. It arises from the time reversal invariance properties of the wave propagation. Due to this invariance, each wavelet scattered by a series of particles interferes constructively with its time reversed counterpart in the backscattering direction, while, sufficiently away from this direction, the interferences average to zero. This results in a backscattering peak having a width proportional to λ/l^*, where λ is the wavelength and l^* is the transport mean free path [2, 8, 11]. CB of light has widely attracted interest because of its connection with weak localization of electrons [12], and also in its own right as a precursor of strong localization of light in very disordered media [13]. In view of the search for the latter regime, it is important to understand well the physics underlying the coherent backscattering. The aim of this study is therefore to compare as far as possible precise measurements of the coherent peak characteristics with recent theoretical predictions [11, 14-16].

The phase shift between a given light path and its time reversed partner is proportional to the product θd, where θ is the angle with respect to the backscattering direction and d the distance between the first and last scatterers of the path [3, 11]. It is therefore a result of all theories [10, 11, 14-17], that the contribution of a given path to the coherent peak extends into an angular range related to the size of the path, i.e. it becomes narrower as the path length,

and hence d, becomes longer. This behaviour can be probed in several ways, for example by time-resolved measurements using pulse technics [18]. As this typically requires a picosecond time scale, we found simpler to study the sensitivity of the peak to addition of an absorbing dye. Since the (long) paths suppressed by absorption at small dye concentrations are much larger than the transport mean free path, our data can be described in terms of the scalar diffusion approximation [11, 15]. Our results also qualitatively agree with the recent measurements of Van Albada *et al.* [19], who studied finite size slabs on the same purpose.

An other basic prediction of all current theories is that the enhancement factor precisely in the backscattering direction ($\theta = 0$) should be exactly 2, when the incident and the detected polarization are parallel [2, 3, 11, 15]. Of course, the possible contribution of single scattering has to be subtracted, as it is not subject to CB. As apparently this factor of two has not been yet precisely reached experimentally, it is of interest to test carefully this point.

Finally, we are also interested in the shape of the CB peak. Both experiments and theory [1-3, 11, 14] have shown that this lineshape depends on the configuration of the polarizers. When detected and incident polarizations are parallel there is full coherence [15] between a light path and its reversed partner. In contrast, in the crossed ($\perp$) configuration, the coherence decays exponentially with the path length [11], resulting in a more complicated situation. Several theoretical approaches have been recently used to predict the lineshape. One of them [10, 16] is exact for scalar waves, and can thus be applied, at best, only to the parallel ($/\!/$) configuration of polarizers. Another [14] takes fully into account the vectorial character of light, but relies on a diffusion approximation. Both of these approaches deal with point-like scatterers. However, the coherent backscattering effect is by no means restricted to such a simple case. Most natural media are polydisperse suspensions — or solids — of scatterers with size comparable to the wavelength. In this case, one may presently rely on the approximate, but simple, results of the scalar diffusion theory [11, 15] which should be valid for angles θ smaller than λ/l^*. This theory predicts that, once θ is scaled by λ/l^*, the ($/\!/$) peak lineshape should be universal and have a triangular singularity at small angles [11, 15]. Accordingly, lineshape measurements should yield the transport mean free path l^* of light in the medium and may help to its characterization. Therefore, we found useful to test these predictions and their angular range of validity as a function of the size of scatterers, using as well defined media suspensions of calibrated monodisperse polystyrene spheres.

The data presented here, obtained using an improved experimental set-up (Sect. 2) provide evidence that a simple diffusion theory correctly describes, i) the effect of absorption due to an added dye (Sect. 3) and ii) the shape of the $/\!/$ backscattering peak as a function of the single parameter λ/l^* (Sect. 5). Results on the enhancement factor in the backscattering direction and on the $\perp$ lineshape are presented in sections 4 and 5, respectively. We finally report in section 6 data on the statistics of the multiply scattered intensity fluctuations, a subject which recently became of interest [5, 6, 20].

2. Experimental set-up.

The experimental set-up used was similar to the one described earlier [3, 20], with some modifications made in order to improve the angular resolution. A low divergence (< 0.6 mrd) Ar laser beam was reflected from an optical quality slightly wedged (30′) glass slide onto the sample. Thereby, angle dependent interferences in the measured signal (due to double reflection from the slide) were avoided. The slide was oriented nearly normally to the backscattering direction ($\sim 15°$ off) so that its transmission did not significantly depend on the angle of observation or the polarization of detected light. For the same reason and also because this geometry simplifies the theoretical predictions, the sample was *quasi* normal to the backscattered direction (a tilt of less than five degrees was enough to avoid specular reflection towards the detector). Extrascattering by the slide in the backscattering direction was suppressed by chopping the light scattered from the sample and using lock-in detection. The additional small scattering from the darkened chopper blades could be measured in the absence of sample and subtracted from the signal with sample. This procedure was particularly advantageous for measuring the small variations of the peak lineshape due to added dye. The sample to detector distance was increased up to 2 m and smaller pinholes used (0.5 mm diameter, at respectively ~ 1 and ~ 2 m from the sample). The corresponding geometrical resolution was about 0.25 mrd HWHM, or 1 mrd total width. The illuminated region of the sample was chosen sufficiently small (2 mm diameter) so that the overall resolution was hardly affected by diffraction from the pinholes. It was experimentally measured to be ~ 0.3 mrd HWHM, by replacing the sample by a properly aligned mirror (note that this result includes the effect of the divergence of the incident beam). The time constant of the lock-in output was set to 10-30 s, so that the Brownian motion of the spheres properly integrates out the speckle noise [5, 6] (the typical correlation time of which is ≈ 1 ms [20]). This sets an upper limit of $\sim 10^{-2}$ mrd/s for the scanning rate of the goniometer arm. The samples

were aqueous suspensions of polystyrene spheres (diameter 0.109, 0.305, 0.46, 0.797 μm) purchased from Sigma Corp. In order to obtain a smooth backscattering peak, the samples were sonified and gently centrifugated before the experiment. This eliminated the few large aggregates of beads, which tend to appear after several days, but did not significantly change the solid fraction. Finally, for all results reported here, the direction of incident polarization was kept normal to the plane of scan. This is important for the smallest scatterers, for which an anisotropic peak shape has been recently observed [19].

3. The effect of absorption.

In order to study the effect of a finite inelastic scattering length, an absorbing dye was progressively added to a 10 % solid fraction suspension of 0.46 μm diameter polystyrene spheres. A nearly saturated stock solution of Rhodamine 6G (R6G) in methanol was used because the absorption at a wavelength in water $\lambda_w = 0.515/1.33 = 0.389$ μm is large and does not vary with light exposure time. The absorption mean free path l_a of a given sample was determined by measuring the transmission of an aqueous solution with identical dye concentration (we assume that the dye absorption is not affected by the presence of polystyrene spheres). The largest dye concentrations studied were about 10 %, corresponding to $l_a \sim 100$ μm (above 20 % of dye, the polystyrene beads tended to agglomerate). The variation of l^* due to dilution with dye solution was thus small and the observed variation of the peak shape essentially resulted from the change in l_a.

Figure 1 shows the scattered intensity near backscattering for a pure and two absorbing samples, in both parallel (a) and crossed (b) configurations of the polarizers. The following observations can be made :

i) The reduction, due to the dye, of the incoherent intensity (i.e. the intensity outside the peak) is identical for both (//) and (⊥). As only the longest paths are suppressed by the dye, this observation shows that their contribution to the incoherent intensity is fully depolarized, as expected.

ii) The // coherent signal (peak intensity *minus* incoherent background) is decreased by about the same factor than the incoherent signal, whereas the (⊥) coherent signal is much less affected. This demonstrates that, without dye, all loops contribute to the // coherent backscattering, but only small paths are involved in the ⊥ coherent backscattering.

iii) The shape of the // peak is modified, i.e. it progressively flattens as the dye concentration is increased. This is because the longer paths, which contribute only to smaller angles of the peak, are eliminated. Similar results, obtained by studying finite slabs, have been recently reported by Van Albada *et al.* [19].

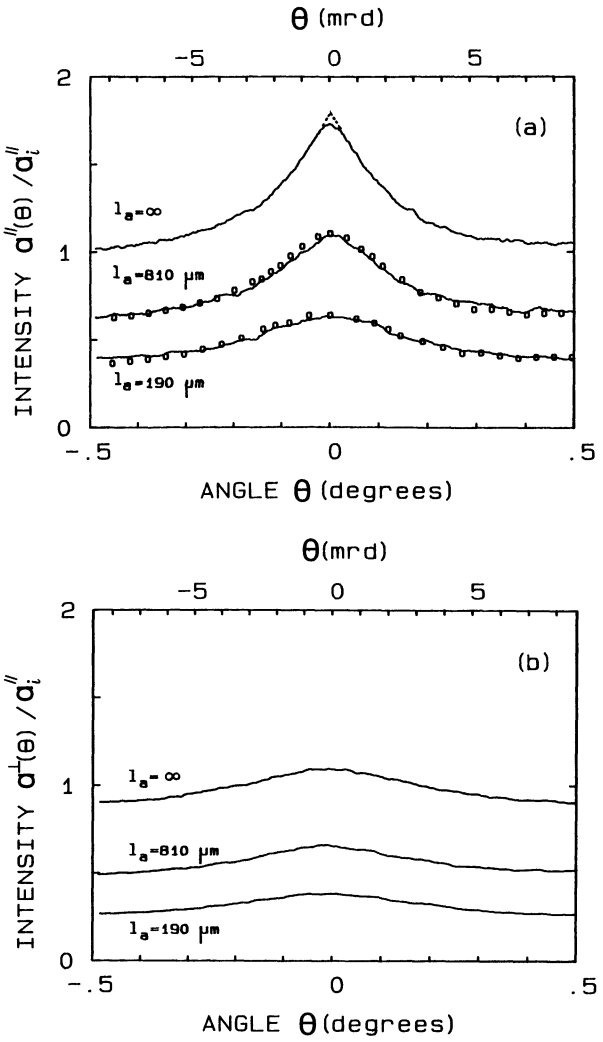

Fig. 1. — (a) Dependence of the coherent backscattering effect on absorption for parallel polarizers. The sample is a 10 % solid fraction aqueous suspension of 0.46 μm diameter polystyrene spheres, with dye added (absorption mean free path l_a). The scattered light intensity $\alpha^{\parallel}(\theta)$ is normalized by its value $\alpha_i^{\parallel}$ at 1° for the pure sample ($l_a = \infty$). The dots are the predictions of the diffusion theory for samples with dye, as derived from the curve for the pure sample (see text) ; (b) The same as (a), but for crossed polarizers.

After this qualitative discussion, we proceed to a quantitative analysis of the above observations. Because of point i) above, we expect the scalar diffusion theory [7, 15] to be valid for the suppressed paths. According to this theory, the coherent part of the albedo is given by an integral [7, 15]

$$\alpha_c(q, l_a) = \iint P(r, L)\, C(L) \exp(-L/l_a)\, dL \times \times \exp(i\mathbf{qr})\, d^2\mathbf{r}$$

with $q = 2\pi\theta/\lambda$, where θ is the angle of observation with respect to backscattering measured, as λ, in air and l_a is the absorption mean free path. $P(r, L)\exp(-L/l_a)$ is the weight of paths of length L, the ends of which are a distance r apart, in a direction parallel to the interface. $C(L)$ is the coherence ratio for paths of lengths L, which equals 1 in the (//) configuration, but decays with L in the ($\perp$) configuration ([1]).

In the diffusion approximation, P depends on r through the Gaussian $[\exp(-3r^2/4Ll^*)]/Ll^*$ so that

$$\alpha_c(q, l_a) = \int \exp(-q^2 Ll^*/3 - L/l_a)\, C(L)\, P_1(L)\, dL$$

where $P_1(L)$ is a function of L only. We thus directly obtain

$$\alpha_c(q, l_a) = \alpha_c([q^2 + q_a^2]^{1/2}, \infty) \quad (1)$$

where

$$q_a^2 = 3/(l_a l^*)\,. \quad (2)$$

Equation (1) relates the albedo in the case of absorption to the albedo without absorption, for any configuration of polarizers. Note that this relation does not depend on the boundary conditions for the diffusion equation, which only determine $P_1(L)$. In the backscattering direction ($\theta = q = 0$), we have

$$\alpha_c(0, l_a) = \alpha_c(q_a, \infty)\,. \quad (3)$$

By comparing the experimental lineshape with and without absorption, we determine for each l_a an angle θ_a and hence $q_a = 2\pi\theta_a/\lambda$, using (3). Physically, θ_a corresponds to the width of the central part of the CB peak due to those long loops ($L > l_a$) that have been suppressed by absorption [15, 17]. Figure 2 shows the obtained values of q_a plotted as a function of $(1/l_a)^{1/2}$. q_a appears indeed proportional to $(1/l_a)^{1/2}$ as predicted by (2). From the slope of the best linear fit through the data, we find for the transport mean free path a value of

$$l^* = 20 \pm 2\ \mu m$$

in agreement with the estimation $l^* \sim 20\ \mu m$ given in appendix A. In addition, equation (1) appears valid not only for $q = 0$, but also for the whole q range of interest, as shown by the dots in figure 1a. These dots correspond to

$$[\alpha_i(l_a) + \alpha_c((q^2 + q_a^2)^{1/2}, \infty)]$$

([1]) We here assume that $C(L)$ depends only on L. This should be true for large enough L ($L \gg r$).

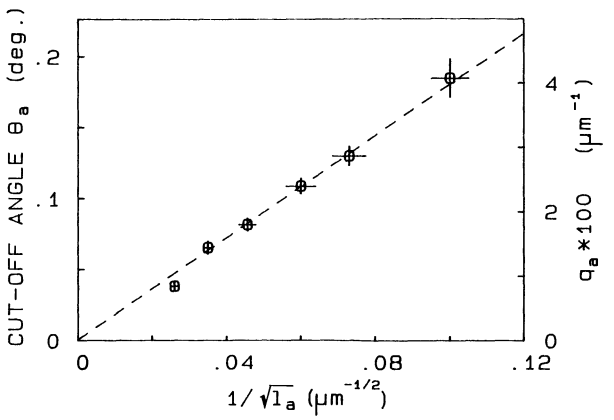

Fig. 2. — Dependence of the experimental cut-off angle θ_a ($q_a = 2\pi\theta_a/\lambda$) on the absorption mean free path l_a. The dashed line is the theoretical prediction for a transport mean free path $l^* = 20\ \mu m$.

where both the incoherent albedo $\alpha_i(l_a)$ and $\alpha_c(q, \infty)$ are experimentally measured, and q_a is calculated using (2) from l_a and $l^* = 20\ \mu m$. They are very close to the experimental curves $\alpha_i(l_a) + \alpha_c(q, l_a)$. Hence, in the range of l_a studied (down to about $120\ \mu m \cong 6\, l^*$), the scalar diffusion theory correctly accounts for the effect of absorption on the coherent backscattering peak.

We shall see that this theory also accounts for the *absolute* variation of the incoherent albedo $\alpha_i(l_a)$ with the absorption mean free path l_a. This variation is related to the angular dependence of the coherent // albedo

$$\alpha_i(\infty) - \alpha_i(l_a) = \alpha_c^{\parallel}(0) - \alpha_c^{\parallel}(q_a) \quad (4)$$

where q_a is connected to l_a through (2). For large l_a (small q_a), we have for each polarization

$$\alpha_i(\infty) - \alpha_i(l_a) = -\frac{d\alpha_c^{\parallel}}{dq_a}(0) \cdot q_a = \beta l^* q_a/2 \quad (5)$$

where the factor 1/2 accounts for the observation of a given polarization and β is a constant which was derived earlier [11, 15]

$$\beta = \frac{3F_0}{4\pi}\left(1 + \frac{z_0}{l^*}\right)^2 \quad (6)$$

where $z_0/l^* \approx 2/3$ is fixed by the boundary condition on the diffusion equation [15, 22]. F_0 and α are the incident homogeneous flux and the diffused flux (per unit solid angle) respectively. Figure 3 shows the variation of the experimental value of α_i with $(1/l_a)^{1/2}$ for both polarizations. Consistent with figure 1, the two curves are found nearly parallel, up to the largest dye concentrations used. This shows that, at least for the paths longer than about $6\, l^*$, the light is fully depolarized by the multiple scattering. Furthermore, the variation of α_i is linear

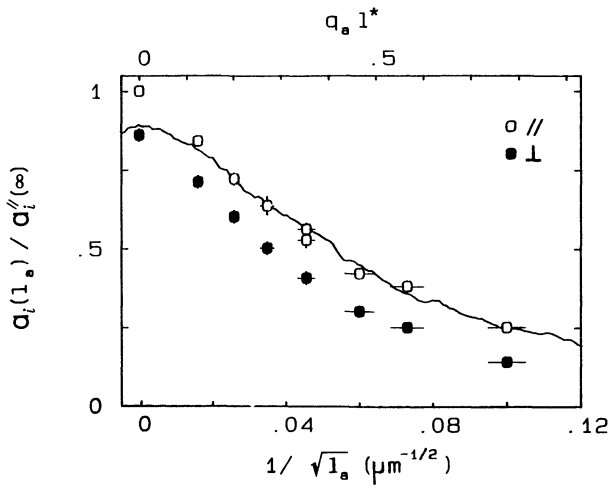

Fig. 3. — Dependance of the incoherent intensity α_i (measured at 1° and normalized by the pure // incoherent intensity $\alpha_i^{//}$) on the absorption mean free path l_a, for both polarizers configurations (o and •). The full curve is the experimental // coherent albedo in the pure case, divided by 0.8 (see text).

for small q_a's, as expected from equation (5). We find

$$\alpha_i(l_a) = \alpha_i(\infty)\,(1 - (1.35 \pm 0.15)\,q_a\,l^*) \quad (7)$$

when using $l^* = 20$ μm. We emphasize that the linear dependence of α_i on $(1/l_a)^{1/2}$ is equivalent to the linear angular dependence of the coherent albedo at $\theta \simeq 0$ (triangular singularity). It is however more easily measurable since $\alpha_i(l_a)$ is, unlike $\alpha_c(\theta)$, not sensitive to a finite experimental resolution.

Expression (5) is expected to hold quantitatively since it depends only on the contribution of long paths [15]. This can be experimentally tested from (7), provided the absolute value of $\alpha_i(\infty)$ is known. To this end, we have calibrated our detector by measuring the signal of dilute samples of nearly point-like scatterers (0.109 μm diameter) which can also be computed. For the 10 % solid fraction pure suspension of 0.46 μm beads, we then find $\alpha_i^{\parallel} \approx 3.1 \pm 0.3\,F_0/4\pi$ ([2]). Inserting this value in (7), we obtain $d\alpha_i/d(q_a l^*) = -4.2\,F_0/4\pi$ (± 20 %), in good agreement with the predictions (5) and (6) since $\beta/2 \approx 4.2\,F_0/4\pi$. Note that this agreement depends through β on the value chosen for z_0. In particular it could not be obtained with the simple choice $z_0 = 0$ [14] (which would give $\beta/2 \cong 1.5\,F_0/4\pi$).

([2]) For the 0.109 μm beads at a 10 % solid fraction, we obtain from this calibration $\alpha_i^{\parallel} + \alpha_i^{\perp} \sim (5 \pm 0.5)\,F_0/4\pi$. This is in agreement with the diffusion theory [22] and with the measurements of Kuga and Ishimaru [1]. For the other beads, we find $\alpha_i^{\parallel} + \alpha_i^{\perp} \sim 6\,F_0/4\pi$ (see Tab. I) also in agreement with reference [1].

4. Enhancement factor in the backscattering direction.

From the curve ($l_a = \infty$) in figure 1a, it is obvious that the lineshape is not triangular at small angles and that the enhancement factor at $\theta = 0$ is not two. We shall now discuss possible experimental reasons for this behaviour.

Besides a finite instrumental resolution, any effect limiting the maximal size of coherent paths will round the tip of the ideal triangular lineshape, without necessarily affecting the factor of two enhancement at $\theta = 0$. For instance, absorption or finite thickness D of the sample decrease both the coherent and incoherent intensities by the same amount and hence preserve the factor of two ; the characteristic angles are $\lambda/(l^* l_a)^{1/2}$ or λ/D [17], respectively. In our case (pure sample, cell thickness $D = 1$ cm), these angles are much smaller than our experimental resolution. On the other hand, some effects influence in a different manner the coherent and incoherent intensities. An exemple is the Brownian motion of the spheres, because it breaks the time reversal invariance and hence suppresses the coherent contributions of the largest loops (with a characteristic cut-off angle ([3]) $\lambda/(l^{*3} l_B)^{1/4}$, where $l_B = c\lambda^2/D_B$ with c the velocity of light and D_B the diffusion constant of the spheres). Another example is non uniformity of the incident flux because, in this case, the intensities on time reversed paths are not equal. Both of these effects decrease the value of backscattering enhancement, but in our case by at most 1-2 % of α_i. The main rounding effect is due to finite angular resolution. By two dimensional convolution of the « ideal » dependence corresponding to equation (7) with the measured instrumental profile we find a corresponding decrease of $\alpha_c(0)$ by about 10 %. Hence, the estimated total rounding effect is between 10 % and 12 % of α_i. Adding this correction to the experimental $\alpha(0)/\alpha_i \sim 1.73$, we find an « ideal » backscattering enhancement between 1.80 and 1.85. This estimation is confirmed by the following independant argument.

An interesting feature of the data shown in figure 3 is the validity of the linear regime up to $q_a \sim 0.015\ \mu m^{-1}$ (corresponding to $q_a l^* \sim 0.3$) or equivalently up to $\theta_a \sim 1.3$ mrd, which is an angle larger than the instrumental width in the θ-scan experiments. Thus, the ideal enhancement factor at $\theta = 0$ can be evaluated by linear extrapolation of the backscattering peak without dye from $\theta \sim 1$ mrd down to $\theta = 0$. This procedure, as illustrated in figure 1a, yields again $\alpha_{extr.}(0)/\alpha_i \sim 1.8 - 1.85$,

([3]) This result was established in reference [8] for isotropic scattering ($l^* = l$). Arguments similar to that used in reference [20] show that, for large scatterers, it remains valid with l^* replacing l.

where α_i is measured outside the peak (at $\pm 1°$). It thus seems that, even in an « ideal » situation, the predicted coherent backscattering enhancement of 2 would not be reached. The remaining difference between $\alpha_{extr.}(0)$ and $2\,\alpha_i$ (at least 10 %) cannot be due to single scattering alone neither from the 0.46 μm diameter spheres ([4]) nor from other scatterers (aggregates, dirts, ...). Indeed, this would imply a progressive decrease of the enhancement factor when suppressing the larger paths by addition of dye, which is not observed. Specifically, the enhancement factor would be 1.20-1.40 for the smallest $l_a(\approx 6\,l^*)$ while we measured 1.7 ± 0.1. This suggests that, for any path, the coherence factor is only 0.80-0.85. Consistently the experimental values of $\alpha_c^{\parallel}(q_a, \infty)$ $(\approx \alpha_c^{\parallel}(0, l_a))$ when divided by 0.8 agree fairly well with the experimental values of $\alpha_i(l_a)$ for values of q_a larger than the experimental resolution (Fig. 3).

Hence, our result seems to contradict the theoretical prediction $\alpha_c^{\parallel} = \alpha_i^{\parallel}$. For other materials ([5]) with smaller l^* and higher solid fractions, the enhancement factor also seems to be smaller than two [6, 16]. As pointed out by Lagendijk [21], this effect may be due to multiple scattering contributions neglected in the present theory. In this context, it is interesting to note that the coherent contribution of closed light paths with first and last scattering from the same particle does not depend on angle. On the other hand, Van Albada *et al.* [19] reported, for similar polystyrene spheres, an enhancement factor of two, once the contribution of the first layers of their sample has been subtracted. It is not clear to us that these measurements are precise enough to preclude any enhancement factor larger than 1.8. Moreover, the same authors have recently found that their enhancement was appearently overevaluated [16]. Hence whether our own and others results are still subject to experimental artefacts ([6]) or reveal real effects not yet included in the theory remains an open question. High resolution and beamsplitter free techniques such as recently used by Kaveh *et al.* [6] could help to settle this question.

5. Analysis of the lineshape.

We showed in section 3 that for the finite size scatterers used a scalar diffusion theory [11, 15] accounts for the modification of the lineshape due to absorption, at least down to path lengths of about $6\,l^*$. This theory can thus be expected to give a good description of the coherent peak shape for the pure material up to ql^* values close to unity. In this section we shall confirm this result though, at a first glance, it may seem surprizing since a scalar diffusion theory should be valid ; i) only for $L \gg l^*$, or equivalently $ql^* \ll 1$, even for scalar waves, ii) for vectorial waves, only after a sufficient number of scattering events for the « incoherent » intensity to be fully depolarized.

Concerning i), Van Albada *et al.* [16] have numerically solved the transport equation [10] for the incoherent intensity. They thus obtained the exact order by order contribution to the scattered intensity for a scalar wave and point like scatterers and found that the diffusion approximation carried out in reference [11] is in fact quite good. Concerning ii), Stephen and Cwillich [14] have shown, again for point-like scatterers, that the vectorial nature of light has an important effect on the lineshape ([7]). As discussed in reference [15], the physical mechanism for this effect is the initial transfer of polarization from the incident to the crossed direction. This transfer also results in the prediction of an about two times smaller incoherent intensity in the perpendicular configuration of polarizers than in the parallel one [6]. As shown in the second row table I, this is indeed experimentally observed for small enough scatterers. For larger scatterers, however, where $l^* \gg l$ (see Tab. II), the ratio of both intensities is found close to unity. This depolarization ratio which appears large compared to the case of point like scatterers is likely due to the fact that numerous scattering events occur on a transport mean free path, depolarizing the incoherent intensity for paths of length $L > l^*$. If this is so, a scalar diffusion theory is more relevant for these larger spheres than the vectorial theory derived for point-like scatterers [14].

Consequently, one could expect the lineshape to depend only on ql^*, and not on the microscopic properties of the scatterers. We tested this by plotting in figure 4 the lineshape as a function of a reduced angle θ/θ^*, for the three larger diameters

([4]) Single scattering is responsible for the factor 1.89 instead of 2 found in reference [14] for point-like scatterers. However, for our 0.46 μm diameter spheres, one can estimate this single (Mie) scattering contribution to be less than 1 % of the total backscattered intensity.

([5]) Using a solid sample similar to Kaveh *et al.* [6] ($BaSO_4$ particles), we found extrapolated enhancement factors of 1.7 (see Fig. 8) and 1.1 in the // and ⊥ configurations of polarizers, respectively.

([6]) One may consider the diffused light reflected from the cell walls back into the sample since this process is not governed by the same polarization properties than scattering from spheres. However this process can be shown to also preserve the full coherence between time reverse paths in the parallel configuration (the method is similar to that used in reference [15] to deal with Mie scattering).

([7]) While we feel their diffusion approximation may be somewhat unsuitable for treating this problem, their result is presumably qualitatively correct, as discussed in reference [15].

Table I. — *Compared experimental values of the albedo for* 10 % *solid fraction aqueous suspensions of polystyrene spheres (diameter* 2 *R). The incoherent intensities for both polarizer configurations are normalized by the incoherent // intensity* $\alpha_i^{\parallel}(0.46)$ *for the* 0.46 μm *diameter beads –* θ^* *is the half width at half maximum of the // peak (obtained as described in the text) and* $q^* l^* = 2\pi\theta^* l^*/\lambda$, *where* λ *is the wavelength in air and the transport mean free path is determined in the appendix* (Tab. II). *The enhancement factor in the backscattering direction for crossed polarizers* ($\alpha_c^{\perp}/\alpha_i^{\perp}$) *is also given.*

2 *R* (μm)	0.109	0.305	0.46	0.80	
$\alpha_i^{\parallel}/\alpha_i^{\parallel}(0.46)$	1.07	0.98	1	0.95	(± 0.02)
$\alpha_i^{\perp}/\alpha_i^{\parallel}(0.46)$	0.53	0.90	0.92	0.93	(± 0.02)
$(\alpha_i^{\parallel} + \alpha_i^{\perp})/\alpha_i^{\parallel}(0.46)$	1.60	1.88	1.92	1.88	(± 0.04)
$\alpha_i^{\perp}/\alpha_i^{\parallel}$	0.5	0.92	0.92	0.98	
θ^* (mrd)	0.85	2	1.85	1.45	
$q^* l^*$	0.59	0.41	0.40	0.39	
$\alpha_c^{\perp}/\alpha_i^{\perp}$	0.14	0.21	0.25	0.25	

Table II. — *Calculated transport mean free path* l^* *for* 10 % *solid fraction aqueous suspensions of polystyrene spheres of diameter* 2 *R. The scattering and transport cross sections* σ *and* σ^* *are calculated from Mie theory.* $\rho\sigma l$ *and* $\rho\sigma^* l^*$ *are correcting factors for hard core correlations between spheres (see Appendix A).*

2 *R* [μm]	0.109	0.305	0.46	0.80
$\sigma/\pi R^2$	0.022	0.41	0.99	2.5
$\sigma^*/\pi R^2$	0.019	0.11	0.15	0.21
$\rho\sigma l$	1.67	1.35	1.32	1.28
$\rho\sigma^* l^*$	1.49	1.10	1.06	1.05
l [μm]	57	6.75	4.1	2.7
l^* [μm]	58	20.5	21.5	26.7

studied. θ^* is chosen so that $\alpha_c(\theta^*) = 1.4\,\alpha_i$. The three curves are found very similar. The small deviations near $\theta = 0$ are due the finite experimental resolution, the relative effect of which increases with decreasing linewidth ($\sim \theta^*$). Like in section 4, the

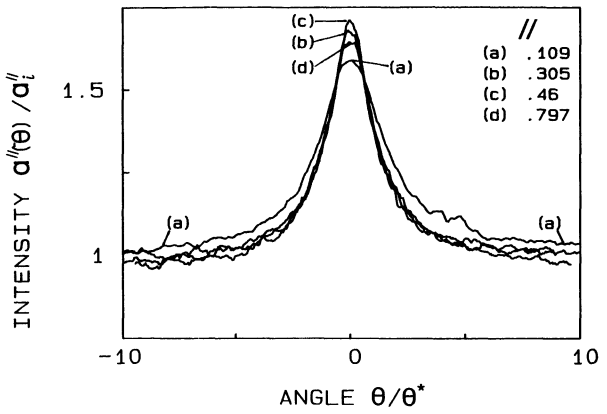

Fig. 4. — // lineshapes for polystyrene spheres of diameters 0.109, 0.305, 0.46, 0.797 μm (solid fraction 10 %). The angles are scaled by the peak widths (θ^*) and the intensities by the multiply scattered // incoherent intensity at 1°.

linear extrapolation of the intensity to $\theta = 0$ appears smaller than $2\,\alpha_i$. In addition, we compare in table I the values of θ^* to theoretical estimates of l^* for the various beads (Appendix A). While $\theta^* l$ strongly varies with the size of scatterers, we find $\theta^* l^* \sim q^* l^* \sim$ const., in full agreement with the prediction of the scalar diffusion theory. Assuming the « ideal » backscattering enhancement to be about 1.8, θ^* is of the order of the half width of half height of the coherent peak. We then note that the value for $q^* l^*$ (~ 0.40) compares well with various theoretical predictions based on the transport equation of intensity for a scalar wave (~ 0.33 [11, 15], 0.36 [16], 0.50 [15]) but is smaller than that of the « vectorial theory » (~ 0.7 [14]). This shows that the transport mean free path of light in a medium containing large enough scatterers can be measured by the width of the coherent backscattering peak ([8]). This property has been recently used [6].

We now compare the full lineshape in the // configuration to the full theoretical prediction of the scalar diffusion theory [11], letting aside for a moment the case of point-like scatterers.

$$\alpha^{\parallel}(q) = \frac{1}{2}\frac{3}{8\pi}\left[1 + 2\frac{z_0}{l^*} + \frac{1}{(1+ql^*)^2}\left(1 + \frac{1 - e^{-2qz_0}}{ql^*}\right)\right] \quad (8)$$

where we have included a factor 1/2 to account for the observation of a given polarization.

([8]) We note however that the incoherent intensity, measured just outside the cone, can considerably depend on the studied material (e.g., we measured it to be 30 % larger for solid $BaSO_4$ than for our polystyrene spheres). Therefore l^* should be better measured from the absolute slope $d\alpha^{\parallel}/dq$ (Sect. 3) than from the width of the peak.

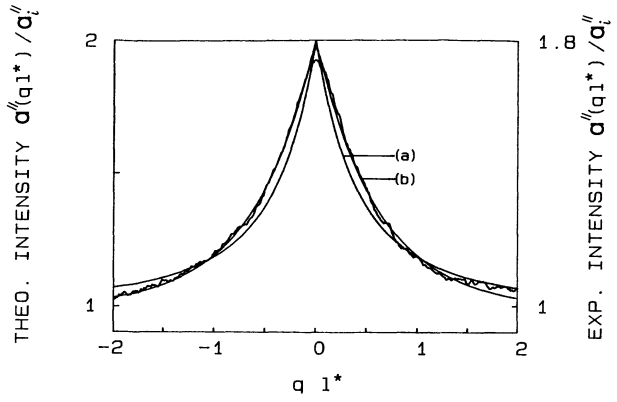

Fig. 5. — Experimental coherent backscattering peak for 0.46 μm polystyrene spheres (solid fraction 10 %) as a function of ql^* ($l^* = 20$ μm). (a) and (b) are theoretical predictions (see text).

Figure 5 shows the experimental lineshape for the 0.46 μm diameter beads plotted as a function of ql^* between -2 and $+2$ (l^* is taken to be 20 μm, as estimated in Appendix A and in agreement with Sect. 3). The (left) vertical scale is chosen such that the linear extrapolation of $\alpha_c^{\parallel}(q)$ at $q = 0$ is 1, instead of 0.8, in units of $\alpha_i^{\parallel}$ (see Sect. 4).

Curve (a), based on equation (8), appears too sharp at small angles. Accordingly, the FWHM of the experimental peak is slightly larger ($2\,q^*\,l^* \sim 0.8$) then predicted by equation (8) (~ 0.66), or by the exact calculation for isotropic scalar scattering [16] (~ 0.72). Since we have shown in section 3 that equation (8) (which implies (5) and (6)) accounts for the absolute slope $d\alpha^{\parallel}/dq$, this merely reflects the fact that the value predicted by equation (8) for

$$\alpha_i^{\parallel} = [3/4(1 + 2\,z_0/l^*)\,F_0/4\,\pi] \sim 1.75\,F_0/4\,\pi$$

is too small when compared to the experimental value $\sim 3.1\,F_0/4\,\pi$ (see Sect. 3).

Curve (b) is based on a slightly different expression, which predicts a better value for α_i. It is calculated as

$$\alpha_c^{\parallel}(q) = \sum_{N=1}^{\infty} \exp(-N(ql^*)^2/3)\,I(N)$$

where $\exp(-N(ql^*)^2/3)$ is the angular dependence of the contribution of the peak of loops of effective order N ($N = L/l^*$) and $I(N)$ is given by :

$$I(N) = \frac{1}{2}\frac{5\,F_0}{8\,\pi}\left[\left(\frac{2}{\pi N}\right)^{1/2}(\exp(-3/4\,N) - \exp(-3(1 + 2\,z_0/l^*)^2/4\,N))\right].$$

The bracketted expression corresponds to a random walk beginning at a distance l^* from the interface and terminating on the interface, with a trapping plane at $-z_0 = -2/3\,l^*$. This choice should be appropriate in the case of large scatterers ($l^* \gg l$). The prefactor $1/2\,5\,F_0/8\,\pi$ is given by the usual diffusion approximation [22] (1/2 accounts for the observation of a given polarization) and is such that the behaviour of $I(N)$ at large N gives the right value of $d\alpha_c^{\parallel}/dq$ (Eq. (5)). With this choice, $\alpha_i^{\parallel} = \sum I(N) \cong 5/2\,F_0/4\,\pi$, the prediction of the usual diffusion approximation [22] for full depolarization, which is closer to the experimental value $3.1\,F_0/4\,\pi$ than (8). This results in a better fit to the experiment (Fig. 5). Although the agreement obtained could be somewhat fortuitous, it shows that the diffusion picture is sufficient to give a good description of the lineshape.

In order to analyse the smallest scatterers (0.109 μm), one has to substract the contribution of single scattering — non negligible in this case — from the scattered intensity. This contribution is estimated (Appendix A) to be about 25 % to 30 %. The experimental line resulting after this subtraction is shown in figure 4 (in this case, θ^* was chosen such that $\alpha_c(\theta^*)$ is 40 % of the multiply scattered incoherent intensity, i.e. $0.28\,\alpha_i$). Whereas this line agrees reasonably well with the lineshapes from the other beads, the corresponding reduced width $q^*\,l^*$ is about 50 % larger than for the other beads. This difference, subject to the estimations of both the single scattering contribution and l^*, could reflect the expected sensitivity of the lineshape, for point-like scatterers, to the transfer of polarization mentionned above.

Since this effect is the basis [15] for the theory by Stephen and Cwilich [14], it is of interest to compare our results to their predictions. As for the FWHM, we find $2\,q^*\,l^* \sim 1.2$ to be compared to 1.35. In addition, their theory predicts a backscattering enhancement of about 1.9, which means a single scattering contribution of 0.1 to be compared to our experimental estimation of 0.25-0.30. The agreement may perhaps be improved by use of a non zero value for z_0 in their theory and by a description of the single scattering better than the one used which relies on the diffusion approximation. However, the recent observation of an anisotropic shape of the peak for polarized incidence [19] makes clear that, in contrast to the case of large scatterers, an exact — analytical or numerical [16] — calculation of the low orders of Rayleigh scattering is necessary to reproduce the // lineshape for point-like scatterers.

Figure 6 shows the lineshape under crossed polarizers for the four different sizes of beads. The scattered intensity was normalized to its value at ± 1° (note that there is no contribution of single scattering in this polarizer configuration) and the angle θ was reduced by the same θ^* than in the // configuration. All four curves have about the same

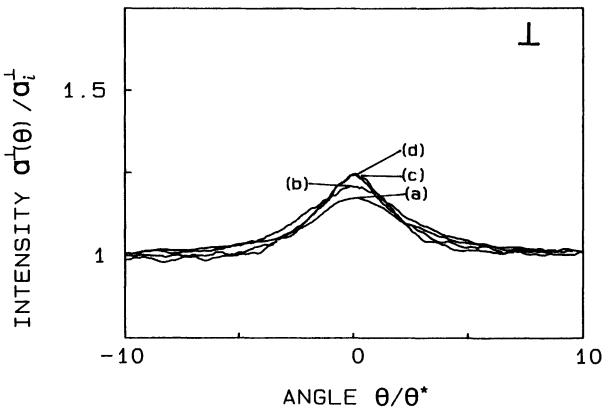

Fig. 6. — Same as figure 4, but for crossed polarizers. The angles are scaled by the same θ^* values as in figure 4 and the intensities by the multiply scattered ⊥ incoherent intensity at 1°.

reduced overall width, which is of the same order than in the // configuration. This is reasonable, since this width is primarily determined by the transverse size of the smallest loops, i.e. l^*. On the other hand, the peak height increases somewhat with the beads diameter as is indicated in the last row of table I.

Thus the crossed lineshape, unlike the parallel one certainly does not have any universal character. Its analysis is complicated by the fact that the coherence factor between time reversed paths is approximately known only for point-like scatterers [11]. We shall thus examine this case first.

As in the case of the parallel configuration, any calculation of the peak width would necessitate an exact calculation of the low orders of Rayleigh scattering. On the other hand, the predictions of Stephen and Cwilich [14] for the depolarization ratio ($\alpha_i^{\perp}/\alpha_i^{\parallel} = 0.4$) and for the coherent enhancement ($\alpha_c^{\perp}/\alpha_i^{\perp} = 0.2$) are in reasonable agreement with the experimental values (0.5 and 0.14 respectively). Such an agreement is also found for a simpler calculation of these two quantities, according to

$$\alpha_i^{\perp}/\alpha_i^{\parallel} = \frac{\sum P(N)\, I(N)}{\sum (1 - P(N))\, I(N)} \tag{9}$$

$$\alpha_c^{\perp}/\alpha_i^{\perp} = \frac{\sum P(N)\, I(N)\, C(N)}{\sum P(N)\, I(N)} \tag{10}$$

where I ($N = L/l^*$) is the scalar contribution (Eq. (8)) of loops of (effective) order N (the lower bound $N = 1$ corresponds to double scattering), $P(N)$ and $C(N)$ are the average intensity weight $I_{\perp}(N)/(I_{\perp}(N) + I_{\parallel}(N))$ and the coherence ratio [15], respectively, of the transverse polarization for these loops. For the smallest beads, we use expressions of reference [15] for $P(N)$ and $C(N)$

$$(P(N) = [1 + 2(0.7)^N]/[2 + (0.7)^N]$$

$$C(N) = 1.5[(0.7)^N - (0.5)^N]/[1 - (0.7)^N])$$

and find $\alpha_i^{\perp}/\alpha_i^{\parallel} = 0.64$, $\alpha_c^{\perp}/\alpha_i^{\perp} = 0.14$, which also compare fairly well with the experimental values 0.7 ([9]) and 0.14. This agreement makes conceivable that expression (10) indeed gives a good approximation of the backscattering enhancement for crossed polarizers.

On this basis, we may compare the prediction (10) to the experimentally measured $\alpha_c^{\perp}/\alpha_i^{\perp}$ for large scatterers. In this case, $P(N > 1) \sim 1$, as previously discussed, but $C(N)$ is not known. However, it is interesting that, taking $P(N) = 1$ and assuming than $C(N)$ is given by the expression derived for point-like scatterers, we find $\alpha_c^{\perp}/\alpha_i^{\perp} = 0.27$ in surprizingly good agreement with the experiment. This would suggest that unlike the polarization, the coherence between time-reversed paths in the crossed configuration pertains over distances of order l^* rather than l. This is consistent with figure 1b, which shows that even for $l_a \approx 7\, l^*$, the height of the ($\perp$) peak is reduced compared to the pure case ($l_a = \infty$). At any rate, this discussion shows that the crossed lineshape is certainly a less good probe of l^* than the parallel one. This conclusion is reenforced by the fact that some solid samples [6] although made of large scatterers have only a small ⊥ backscattering enhancement ([5]).

6. Statistics of the multiple scattered light.

Recently, Kaveh *et al.* [6] have measured the probability density $P(I)$ of the intensity scattered from a $BaSO_4$ solid sample (for parallel polarizers). They found that $P(I)$ strongly deviates from the usual negative exponential [23] statistics for single scattering Gaussian speckle $P(I/\bar{I}) = e^{-I/\bar{I}}/\bar{I}$, both at backscattering and in the wings of the cone. Their data are better described by the gamma density distribution [23] :

$$\bar{I} P(I/\bar{I}) = \mu^{\mu}/\Gamma(\mu)(I/\bar{I})^{\mu - 1} \exp(-\mu I/\bar{I}) \tag{11}$$

with $\mu = 2.5$. The authors relate this observation to the large value of λ/l^*, corroboting this with numerical simulations. This interesting result appears somewhat surprizing since, at least for uncorrelated scatterers, the multiply scattered fields are

([9]) Since $N = 1$ in Eqs. (9) and (10) corresponds to double scattering (instead of simple scattering in Ref. [15]), $\alpha_i^{\parallel}$ in Eq. (9) does not include single scattering. The indicated value of 0.7 for $\alpha_i^{\perp}/\alpha_i^{\parallel}$ is correspondingly obtained from that given in table I by substracting from the experimental $\alpha_i^{\parallel}$ the estimated single scattering contribution ($\approx 30\,\%$, see Appendix).

believed to be random *independent* variables (except between a given scattering sequence and its time reverse). One would thus expect Gaussian statistics for the total scattered field and consequently a negative exponential statistics ($\mu = 1$) for the intensity. We therefore measured the statistics of $P(I)$ for different systems, specifically on our aqueous suspensions of polystyrene spheres and on different $BaSO_4$ samples. To this end, we analysed the temporal fluctuations of I as arising from Brownian motion and from rotation of the samples, respectively, using a digital 64 channels correlator [20].

It is easy to show for a gamma density distribution of I that $\overline{I^2}/\bar{I}^2 = (\mu + 1)/\mu$, so that one can extract μ from a measurement of the second moment of I. This quantity can be measured even for a small number n of photocounts *per* sampling time by extrapolation of

$$\overline{I(0)\,I(t)}/\overline{I(0)}^2 = \overline{n(0)\,n(t)}/\overline{n(0)}^2$$

to zero time [24]. For all our polystyrene suspensions at a 10 % solid fraction, we find $\overline{I^2}/\bar{I}^2 \sim 1.77$ or $\mu \sim 1.3$. The difference between $\mu = 1.3$ and the theoretical value 1 for Gaussian statistics is what usually occurs in correlation spectroscopy experiments because of finite angular resolution ([10]). We observe the same value $\mu \sim 1.3$ for dilute samples in the single scattering regime ($\lambda/l^* \ll 1$) and also for a sample of 0.305 μm diameter spheres concentrated up to a solid fraction of about 20 % by centrifugation ($l^* \sim 9$ μm as determined from its backscattering peak). In the latter case $\lambda/l^* \sim 0.05$, which is only two times smaller than the values in the experiment by Kaveh *et al.* The second moment of our intensity in all regimes including the strongly multiple scattering regime is thus consistent with the usual negative exponential law for $P(I)$.

In addition, we directly measured the full statistics $P(n)$ of photocounts for various suspensions of polystyrene beads. To this end one has to use a sample time τ short enough to essentially deal with a « solid » sample over a time τ, i.e. $\overline{I(0)\,I(\tau)} \cong \overline{I^2(0)}$. For the 0.46 μm diameter spheres in water, τ must be smaller than 5 μs in order to have $\overline{I(0)\,I(\tau)}/\overline{I^2(0)} > 0.9$ because of the fast short time decay of $\overline{I(0)\,I(t)}$ observed earlier [20]. As the long time relaxation time of $\overline{I(0)\,I(t)}$ is of order 1 ms [20], we can acquire statistics on about 10^5 independent samples in a hundred second experiment ! Unfortunately, our electronic detection system is not suited for average photon count rates larger than 3×10^5/s, corresponding to ~ 0.15 per sample time. At small number of photocounts *per* sample time τ the statistics of $P(n)$ is dominated by the Poisson statistics of the photomultiplier. For the statistics of $P(I)$ given in equation (11), the Mandel formula [26] relating $P(n)$ and $P(I)$ yields

$$P(n) = \frac{\bar{n}^n}{(\mu + \bar{n})^{\mu+n}}\,\mu^{\mu}\,\frac{\Gamma(n+\mu)}{n!\,\Gamma(\mu)} \qquad (12)$$

$\bar{n}$ being the average number of photons *per* sample.

In order to obtain a reliable value for μ from equation (12), one needs $\bar{n} > 1$. We therefore increased the viscosity of our samples by adding glycerol. On adding to a 10 % solid fraction suspension of 0.46 μm diameter spheres an equal amount of glycerol the relaxation times become about 5 times longer and we reached $\bar{n} \sim 4$. Figure 7 shows the measured distribution $P(n)$ obtained under such conditions outside the cone (data were identical for $\theta = 0$). Curves (a) and (b) are computed from equation (12) with $\mu = 1.3$, 2.5 respectively. We again find agreement with $\mu = 1.3$, consistent with the direct measurement of the second moment of I. However, the mean free path of this sample was only ~ 100 μm, due to both dilution and the larger optical index of glycerol compared to water, and hence λ/l^* is about 0.005 i.e. 25 times smaller than in the experiment by Kaveh *et al.*

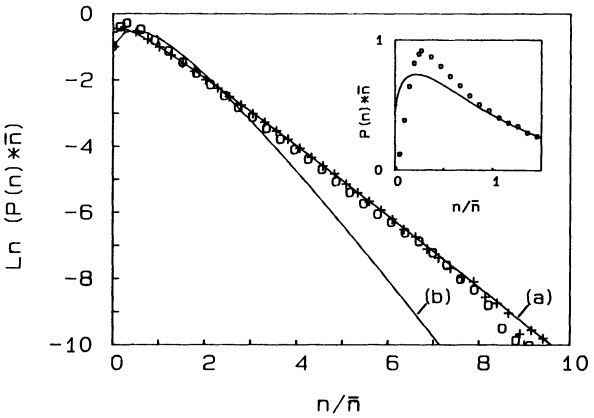

Fig. 7. — Probability density $P(n)$ of photocounts for the intensity scattered by two suspensions of 0.46 μm polystyrene beads. The angle from backscattering is 2°. (+) 5 % polystyrene—45 % water—50 % glycerol ($\lambda/l^* \sim 0.005$, sampling time 25 μs, $\bar{n} = 3.9$) ; (○) 1 % polystyrene—9 % water—90 % glycerol ($\lambda/l^* < 0.001$, sampling time 200 μs, $\bar{n} = 6.6$) ; inset : same sample as (0), but with a sampling time of 1 000 μs and $\bar{n} = 40$ and on a linear scale. Full lines are predictions of equation (12). For $\mu = 1.3$, 2.5 and $\bar{n} = 3.9$ and for $\mu = 1.3$ and $\bar{n} = 40$ (inset).

Precise data on $P(I)$ for small $I/\bar{I}$ can be obtained by using large values of $\bar{n}$ (≈ 50). To this end, we further increased the sampling time (and the relaxation time) by using a suspension with 90 %

([10]) For $\mu = 1.3$, $\overline{I^2} = 1.8\,\bar{I}^2$. This value is consistent with an estimation from the results of reference [25].

glycerol (with a calculated $\lambda/l^* < 0.001$). Figure 7 shows that equation (12) with $\mu = 1.3$ again fits the data for $I/\bar{I} > 1$ but not for $I/\bar{I} < 1$ (we shall come back to this last point below).

We have finally taken advantage of our technique for directly comparing the above results with those obtained from a strongly scattering solid medium consisting of $BaSO_4$ microcrystals. Two different samples were used : the first was kindly provided by W. Erb [27]. The second was made by coating a substrate with a commercial $BaSO_4$ suspension (Kodak White Reflectance coating, Lot 6008) and drying with a resulting solid fraction of about 50 %. Both samples showed backscattering enhancement of the scattered light (cf. Fig. 8), with peak widths similar to that reported by Kaveh *et al.* (FWHM ~ 1° corresponding to $\lambda/l^* \approx 0.1$, as scaled from Tab. I). The results reported hereafter were obtained using the first sample, but an identical set of data was acquired with the second one.

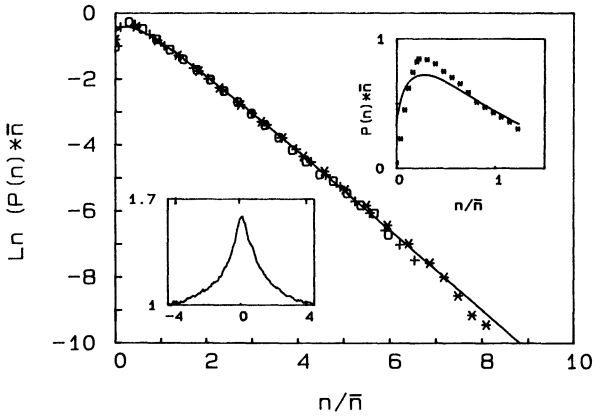

Fig. 8. — Probability density $P(n)$ of photocounts for the intensity scattered by a rotating $BaSO_4$ solid sample ($\lambda/l^* \sim 0.15$) and for parallel polarizers. (○) $\theta = 0°$, $\bar{n} = 11$; (+) $\theta = 0.5°$, $\bar{n} = 9.3$; (*) $\theta = 10°$, $\bar{n} = 6.6$; full line : equation (12) for $\bar{n} = 8$ and $\mu = 1.4$; upper inset : same as (*), but for $\bar{n} = 50$. Full line : equation (12) for $\bar{n} = 50$ and $\mu = 1.4$; lower inset : angular dependance of $I(\theta)/I(5°)$ measured in the same experimental configuration (θ is the horizontal angle — in degrees — with respect to backscattering).

The statistics of the scattered intensity were measured by rotating the sample, again using a sample time τ short enough for the scattered light to remain fully correlated within τ. During the slow rotation, the temporal evolution of the speckle pattern was directly observed on a screen. First, a global rotation around a direction symmetrical to the incident beam with respect to the axis of rotation could be seen. Second, the speckle spots themselves lose their identity. In order to obtain reliable statistics, we therefore slightly tilted the rotation axis ($\approx 5°$) with respect to the incident beam, so that a large number of speckles spots are involved in the measurement of $P(n)$ for all angles of observation studied (between 0° and 10° from the backscattering direction). By measuring the temporal decay of the scattered intensity autocorrelation function, we determined the number of uncorrelated samples used in the determination of $P(n)$ to be between 2 000 and 3 000. The same measurement also gave the maximal allowed sample time τ to deal with a fixed sample. By simultaneous variation of the rotation period and τ, we could obtain $P(n)$ for different n, at a fixed photon flux at the photomultiplier, and alternatively make sure that there was no influence of the incident flux at a given $\bar{n}$ value.

In order to compare $P(I)$ inside and outside the backscattering cone without any extra source of scattered light, we replaced the beamsplitter of section 2 by a mirror at about 1 m distance from the sample. The two pinholes were located between mirror and detector. In this configuration, the overall angular resolution was about 2 mrd and the backscattering direction was missed vertically by about 2 mrd, which is small compared to the FWHM of the backscattering cone. We thus measured $P(n)$ for both polarizer configurations near the backscattering direction ($\theta \approx 0°$), in the wings of the cone ($\theta = 0.5°$) and well outside the cone ($\theta = 4°$ and $\theta = 10°$). Within our experimental precision, we did not find any difference between all these cases (Fig. 8) Unlike in the experiment of Kaveh *et al.* [6], the statistics of $P(n)$ for $I/\bar{I} > 1$ are well represented by equation (12) derived from a gamma density distribution with $\mu \sim 1.3$-1.4. Consistently, the quantity $\overline{I^2}/\bar{I}^2$ measured from the zero time extrapolated autocorrelation function is found ≈ 1.70 to 1.75. Again, this is in agreement with the hypothesis of Gaussian distribution of scattered fields, combined with a non ideal experimental resolution (which was slightly less for these measurements than for those on polystyrene beads reported above). As shown in the inset of figure 8, the data obtained for small $I/\bar{I}$ cannot be fitted by equation (12) with $\mu \sim 1.3$, nor by any other μ, but we recall that this was equally true in the case of the weakly scattering dilute latex sample ($\lambda/l^* \ll 0.001$, inset in Fig. 7). Hence, this behaviour is not due to the relatively large value of λ/l^* for the $BaSO_4$ sample. It can also not be due to dead time problems because the measured $P(n)$ for a given $\bar{n}$ does not depend on the flux incident on the photomultiplier. It seems rather possible that the intensity probability distribution in the case of a slightly non ideal resolution is not perfectly accounted for by a gamma density distribution at small $I/\bar{I}$ [23]. Indeed, on improving the angular resolution for $\theta = 10°$ by

locating the first pinhole near the sample, we obtained data somewhat closer to the ideal negative exponential. This was more obvious on the ratio $\overline{I^2}/\bar{I}^2$ which was found in this case to be ≈ 1.80-1.85 instead of 1.70-1.75. Note finally that by directly fitting $P(n)$ by a gamma density distribution, we would find, as Kaveh *et al.*, a value of μ larger than 1.3, due to the dominant weight of the « anomaly » at small $I/\bar{I}$. However, our large statistics about the large $I/\bar{I}$ behaviour allow us to preclude such a value.

In conclusion, the experiments described in this section reveal no influence (in the range yet explored) of the parameter λ/l^* on the statistics of multiply scattered light, which are always found close to a negative exponential.

7. Conclusion.

We have extensively studied the coherent backscattering effect for light, using aqueous monodisperse suspensions of polystyrene microspheres. We described the sensitivity of the shape of the backscattering peak to the size of scatterers, to absorption and to the polarization of the detected light.

Adding an absorbing dye selectively probes the contribution of long light paths inside the medium to the coherent backscattering peak. Our results show that this contribution is restricted to the central part of the backscattering cone and is significant only for parallel detected and incident polarizations. The progressive rounding of the // peak with increasing absorption is quantitatively accounted for by a scalar diffusion theory. The product of peak linewidth and transport mean free path l^* turn out to be the same for all sizes of spheres studied (except for the smallest ones), again in agreement with such a theory.

In contrast with the present theories, we find an enhancement factor in the backscattering direction between 1.8 and 1.9, once all corrections are accounted for, instead of 2. The reason(s) for this disagreement remain(s) unclear.

Finally, both inside and outside the backscattering cone, Gaussian statistics of the scattered light are observed, in agreement with the usual central limit hypothesis for random independant scattered fields.

This study was restricted to λ/l^* values smaller than 0.15. It appears very interesting to investigate both transport and statistics of the light intensity at λ/l^* values approaching unity. Higher values can be obtained by using spheres of large refractive index (TiO_2 or diamond, for example) but whether this would allow observation of strong localization of light (anticipated for $\lambda/l^* \approx 2\pi$) or possible departure from Gaussian statistics is still an open question.

Appendix A. Determination of the transport mean free path l^*.

We have computed the Mie scattering and transport cross sections σ and σ^* of our polystyrene spheres under our experimental conditions (refractive index of water 1.33, of polystyrene 1.59, wavelength in water 0.387 μm). The scattering mean free path measured from the transmission of diluted samples [3] is within 10 % in agreement with the calculated σ (using a solid fraction 0.1 of the pure sample as given by the manufacturer). For such a large solid fraction, the scattering and transport mean free paths must be corrected due to the hard-core correlations between spheres [19]. We evaluated the correction factors for l and l^* by :

$$\rho\sigma l = \frac{\int \sigma(\omega, \varphi)\, d\varphi \sin\omega\, d\omega}{\int S(\omega)\, \sigma(\omega, \varphi)\, d\varphi \sin\omega\, d\omega}$$

$$\rho\sigma^* l^* = \frac{\int \sigma(\omega, \varphi)(1 - \cos\omega)\, d\omega \sin\omega\, d\omega}{\int S(\omega)\, \sigma(\omega, \varphi)(1 - \cos\omega)\, d\varphi \sin\omega\, d\omega}$$

where ρ is the concentration of spheres, $\sigma(\omega, \varphi)$ the differential cross section, ω the angle between the incident and scattered wavevectors, φ the angle between the plane of (single) scattering and the incident polarization, $S(\omega)$ the static structure factor ([11]) of an hard core interacting gas [28]. The obtained values are given in table II. The correlations substantially increase the scattering mean free path with respect to the « bare » value $1/\rho\sigma$, especially for the smallest beads, in agreement with experiments by Ishimaru and Kuga [29].

Since $S(\omega)$ differs mostly from 1 for small ω, l^* is less affected than l by the finite concentration effect, and the correction is significant only for the smallest beads. The final estimation for l^* is given in last row of table II.

The correlation effect is important for determining the single scattering contribution α_{ss} of the pure 0.109 μm sample. For a given incident flux, it is related to the measured scattered intensity α_d by a dilute sample (mean free path l_d) by

$$\alpha_{ss} = \alpha_d [2/(1 - \exp(-2D/l_d))]\, S(\pi)\, \rho\sigma l$$

where D is the cell thickness. The factor $S(\pi)\, \rho\sigma l$

([11]) The use of the bulk $S(\omega)$ makes sense since we have $l \gg R$, except for the larger beads ($l/R \sim 3$) for which the final correction to l^* is anyway small.

arises from the hardcore correlation. $S(\pi)$ corrects the backward cross-section and $\rho\sigma l$ is the correcting factor to the scattering mean free path l of the pure sample. This correcting factor is important (~ 1.3 since $S(\pi) \sim 0.8$ for a 10 % solid fraction solution). The obtained value for α_{ss} is about 25 % of the measured total ($/\!/$) scattered intensity of the pure (10 % solid fraction) sample.

Note added in proof: the role of absorption has also been recently studied by Etemad *et al.* [30], with results qualitatively similar to ours.

References

[1] KUGA, Y., ISHIMARU, A., *J. Opt. Soc. Am. A* **1** (1984) 831 and
KUGA, Y., TSANG, L., ISHIMARU, A., *J. Opt. Soc. Am. A* **2** (1985) 616.

[2] VAN ALBADA, M. P., LAGENDIJK, A., *Phys. Rev. Lett.* **55** (1985) 2692.

[3] WOLF, P. E., MARET, G., *Phys. Rev. Lett.* **55** (1985) 2696.

[4] EGAN, W. G., HILGEMAN, T., *Appl. Opt.* **15** (1976) 1845.

[5] ETEMAD, S., THOMPSON, R., ANDREJCO, H. J., *Phys. Rev. Lett.* **57** (1986) 575.

[6] KAVEH, H., ROSENBLUH, M., EDREI, I., FREUND, I., *Phys. Rev. Lett.* **57** (1986) 2049.

[7] TSANG, L., ISHIMARU, A., *J. Opt. Soc. Am. A* **1** (1984) 836.

[8] GOLUBENTSEV, A. A., *Zh. Eksp. Teor. Fiz.* **86** (1984) 47 [*Sov. Phys. JETP* **59** (1984) 26].

[9] AKKERMANS, E., MAYNARD, R., *J. Phys. Lett.* **46** (1985) L1045.

[10] TSANG, L., ISHIMARU, A., *J. Opt. Soc. Am. A* **2** (1985) 1331 and *ibid.* **2** (1985) 2187.

[11] AKKERMANS, E., WOLF, P. E., MAYNARD, R., *Phys. Rev. Lett.* **56** (1986) 1471.

[12] LARKIN, A. I., KMELNITISKII, D. E., *Sov. Phys. Usp.* **25** (1982) 185 and
BERGMANN, G., *Phys. Rev. B* **28** (1983) 2914.

[13] JOHN, S., *Phys. Rev. B* **31** (1985) 304 ;
ANDERSON, P. W., *Philos. Mag. B* **52** (1985) 505 ;
ARYA, K., SU, Z. B. and BIRMAN, J. L., *Phys. Rev. Lett.* **57** (1986) 2725 ;
SHENG, P., ZHANG, Z. Q., *Phys. Rev. Lett.* **57** (1986) 1879 ;
GENACK, A. Z., *Phys. Rev. Lett.* **58** (1987) 2043.

[14] STEPHEN, M. J., CWILICH, G., *Phys. Rev. B* **34** (1986) 7564.

[15] AKKERMANS, E., WOLF, P. E., MAYNARD, R. and MARET, G., *J. Phys. France* **49** (1988).
AKKERMANS, E., Thèse de Doctorat, Grenoble (1986) (unpublished).

[16] VAN ALBADA, M. P., VAN DER MARK, M. B., LAGENDIJK, A., to be published.

[17] EDREI, I. and KAVEH, M., *Phys. Rev. B* **35** (1987) 6461.

[18] WATSON, G. H., FLEURY, P. A., MCCALL, S. L., *Phys. Rev. Lett.* **58** (1987) 945.

[19] VAN ALBADA, M. P., VAN DER MARK, M. B., LAGENDIJK, A., *Phys. Rev. Lett.* **58** (1987) 361.

[20] MARET, G., WOLF, P. E., *Z. Phys. B* **65** (1987) 409.

[21] LAGENDIJK, A., private communication.

[22] ISHIMARU, A., *Wave propagation and scattering in random media,* vol. 1 (Academic Press, New York) 1978.

[23] See e.g. GOODMAN, J. W. in : *Laser speckle and related phenomena,* Ed Dainty J. C. (Springer Verlag) 1984.

[24] See e. g. JAKEMAN, E. in : *Photon correlation and light beating spectroscopy,* Ed Cummins H. Z. and Pike E. R. (Plenum Press, New York) 1974.

[25] JAKEMAN, E., OLIVER, C. J., PIKE, E. R., *J. Phys.* **A 3** (1970) L45.

[26] MANDEL, L., *Proc. Phys. Soc.* **74** (1959) 233.

[27] Physikalisch-Technische Bundesanstalt (PTB), Braunschweig, FRG.

[28] WERTHEIM, M. S., *Phys. Rev. Lett.* **10** (1965) 321.

[29] ISHIMARU, A., KUGA, Y., *J. Opt. Soc. Am.* **72** (1982) 1317.

[30] ETEMAD, S., THOMSON, R., ANDREJCO, M. J., JOHN, S. and MACKINTOSH, F. C., *Phys. Rev. Lett.* **59** (1987) 1420.